Proc. Natl. Acad. Sci. USA
Vol. 95, pp. 8075–8080, July 1998
Cell Biology

ClC-5, the chloride channel mutated in Dent's disease, colocalizes with the proton pump in endocytotically active kidney cells

WILLY GÜNTHER*, ANKE LÜCHOW*, FRANÇOISE CLUZEAUD†, ALAIN VANDEWALLE†, AND THOMAS J. JENTSCH*‡

*Zentrum für Molekulare Neurobiologie Hamburg (ZMNH), Universität Hamburg, Martinistrasse 85, D-20246 Hamburg, Germany; and †Institut National de la Santé et de la Recherche Médicale Unité 478, Institut Fédératif de la Recherche 02, Faculté de Médecine Xavier Bichat, BP 416, 75870 Paris Cédex, France

Edited by Gerhard Giebisch, Yale University School of Medicine, New Haven, CT, and approved April 29, 1998 (received for review March 4, 1998)

ABSTRACT **Loss-of-function mutations of the ClC-5 chloride channel lead to Dent's disease, a syndrome characterized by low molecular weight proteinuria, hypercalciuria, and kidney stones. We show that ClC-5 is expressed in renal proximal tubule cells, which normally endocytose proteins passing the glomerular filter. Expression is highest below the brush border in a region densely packed with endocytotic vesicles, where ClC-5 colocalizes with the H^+-ATPase and with internalized proteins early after uptake. In intercalated cells of the collecting duct it again localizes to apical intracellular vesicles and colocalizes with the proton pump in α-intercalated cells. In transfected cells, ClC-5 colocalizes with endocytosed α_2-macroglobulin. Cotransfection with a GTPase-deficient rab5 mutant leads to enlarged early endosomes that stain for ClC-5. We suggest that ClC-5 may be essential for proximal tubular endocytosis by providing an electrical shunt necessary for the efficient acidification of vesicles in the endocytotic pathway, explaining the proteinuria observed in Dent's disease.**

Dent's disease is an X-chromosome-linked disease characterized by low molecular weight proteinuria and hypercalciuria (1). As a consequence of hypercalciuria, patients present with kidney stones, nephrocalcinosis, rickets, and eventually renal failure. Dent's disease is caused by mutations in the gene (*CLCN5*) encoding ClC-5 (2), a Cl^- channel predominantly expressed in kidney (3, 4). ClC-5 belongs to the branch of the CLC Cl^- channel family that encompasses also the highly homologous (80% identical) ClC-3 and ClC-4 Cl^- channels (5). Mutations found in Dent's disease were shown to decrease or abolish the Cl^- channel function of ClC-5 (2, 6, 7).

In contrast to the rather variable symptoms of nephrolithiasis and nephrocalcinosis, low molecular weight proteinuria is a constant feature of Dent's disease. It is present already in children (6), and, in a more moderate form, in carrier females (8) who, due to X-chromosome inactivation, express the wild-type ClC-5 on only every other cell. The selective urinary increase of low molecular weight proteins argues against a defect in the glomerular filter and points to a defect in the proximal tubule. The absence of urinary markers of proximal tubular cell damage (8) suggests that proteinuria is not due to a general dystrophic dysfunction of proximal tubular cells.

Epithelial cells of the renal proximal tubule have one of the highest capacities for endocytosis of a broad range of extracellular proteins. Their specialized endocytotic machinery has been studied extensively on the morphological level (9–11). The filter of the renal glomerular membrane retains cells and large proteins, whereas water, salts, small organic molecules, and small proteins (less than roughly 30 kDa) pass into the primary urine. Glucose, amino acids, and proteins are nearly quantitatively removed from the filtrate in the proximal tubule. Proteins are taken up by endocytosis at the brush-border membrane, a process mediated in part by receptors such as gp330/megalin (11). The proteins are then targeted to the lysosomes for degradation.

Probably every eukaryotic cell internalizes extracellular substances, including proteins, by endocytosis (12). Vesicles are progressively acidified along the endocytotic pathway, with the most acidic pH found in lysosomes (13). Intravesicular acidification is essential for several sorting events, and the dissipation of intracellular pH gradients inhibits the overall process of endocytosis (14–16). Protons are actively transported into these vesicles by a V-type H^+-ATPase (17). It needs a parallel conductive pathway for efficient operation (18–20), whose molecular nature has remained elusive.

Here we show that the ClC-5 Cl^- channel is predominantly expressed in the region below the brush border of proximal tubular cells. It colocalizes with the proton ATPase and with endocytosed proteins early after uptake. Electron microscopy shows its presence in vesicles of the endocytotic machinery. ClC-5 is also expressed in intracellular vesicles of acid-transporting intercalated cells of the collecting duct. It again largely colocalizes with the H^+-ATPase, whose presence in the plasma membrane is controlled by endo- and exocytosis. In transfected cells, ClC-5 is present in endocytotic vesicles and colocalizes with rab5, a marker of early endosomes. Our data suggest that ClC-5 is essential for apical endocytosis in proximal tubule cells, probably by providing an electrical shunt for the H^+-ATPase.

MATERIALS AND METHODS

Generation and Characterization of ClC-5 Antisera. Two synthetic peptides, PEP5A (CKSRDRDTHREITNKS-amide) and PEP5E (CQMANQDPESILFN-COOH), were coupled to BSA through their cysteines. Polyclonal antisera were raised in rabbits (two rabbits per peptide) and were purified by affinity chromatography with the respective peptide. Cross-reactivity against the closely related ClC-4 protein was eliminated by depleting activity against the corresponding ClC-4 peptide. Western blots of crude membrane preparations (25 μg per lane) were probed with purified antisera at a 1:1000 to 1:2000 concentration and a chemiluminescence kit (Renaissance, DuPont). To test for cross-reactivity, capped cRNAs of ClC-3, ClC-4, and ClC-5 were each injected into *Xenopus* oocytes as described (21). Three days after injection, oocytes were homogenized and crude membranes depleted of yolk vesicles were analyzed by Western analysis as above (protein from about two oocytes per lane).

The publication costs of this article were defrayed in part by page charge payment. This article must therefore be hereby marked "*advertisement*" in accordance with 18 U.S.C. §1734 solely to indicate this fact.

This paper was submitted directly (Track II) to the *Proceedings* office.
Abbreviation: IC, intercalated cell.
A commentary on this article begins on page 7843.
‡To whom reprint requests should be addressed at: ZMNH, Martinistr. 85, D-20246 Hamburg, Germany. e-mail: Jentsch@plexus.uke.uni-hamburg.de.

Immunohistochemistry. Rat kidneys were perfused through the abdominal aorta for 2 min with 2% paraformaldehyde in PBS, followed by a 5-min perfusion with 18% sucrose in PBS. Kidneys were removed and frozen immediately. Cryostat sections (7 μm) were blocked by 30-min incubation with 2% BSA/0.5% Triton X-100 in PBS. Purified anti-ClC-5 sera were diluted 1:1000 to 1:2000 in PBS and incubated with the sections at 4°C overnight. Goat antibodies to rabbit IgG, coupled to Cy3 or Cy5 dye (Jackson ImmunoResearch), were used as secondary antibodies. Monoclonal antibodies were detected by a Cy2-coupled goat antiserum to mouse IgG. Double labeling using two rabbit antisera involved an intermediate blocking step with normal rabbit serum (diluted 1:20 in PBS) to block the first detection antibody and goat anti rabbit-IgG Fab fragments (diluted 1:50 in PBS). Confocal laser scanning microscopy was performed with a Leica TCS NT system. For electron microscopy, 20-μm cryostat sections of kidneys fixed by intraaortic perfusion with 2% paraformaldehyde were incubated with the PEP5E2 antibody (1:400) for 20 h, followed by biotinylated goat anti-rabbit IgG (Vector) (2 h) and an avidin–peroxidase complex (Vectastain), and finally by an incubation in 0.03% diaminobenzidine/0.015% H_2O_2. Tissue slices were postfixed by 2% OsO_4 and embedded in Durcupan ACM (Fluka). Ultrathin sections were examined with a Philips transmission electron microscope.

Endocytosis in the Proximal Tubule. One milligram of β_2-microglobulin was labeled with Cy5 by using a kit (Amersham). A 25-μg portion of labeled β_2-microglobulin was diluted in 1 ml of PBS and injected into the jugular vein of rats. Kidneys were fixed by perfusion as above at several time points after injection of the protein.

Transfection Studies in COS-7 and MDCK Cells and Endocytosis. cDNAs of human ClC-5 (2), *Torpedo* ClC-0 (22), and rab5 derivates (23) were cloned into the eukaryotic expression vector pFrog3 derived from pCDNA3 (Invitrogen) by flanking the multiple cloning site with 5′ and 3′ untranslated regions from the *Xenopus* β-globin gene. Human rab5a was cloned by reverse transcription–PCR, and the Q79L mutation was inserted by recombinant PCR. For detection using the monoclonal antibody 9E10, rab5 constructs were N-terminally tagged with the myc-epitope (MEQKLISEEDLQS). COS-7 African green monkey kidney cells and MDCK canine kidney cells were transfected by using Lipofectamine (GIBCO), seeded on glass slides treated with aminoalkylsilane, and fixed with 4% paraformaldehyde 36–48 h after transfection. COS-7 cells were incubated for 5 min at 37°C with 20 μg/ml α_2-macroglobulin (Sigma) in Dulbecco's modified Eagle's medium (DMEM) containing 1% BSA. Endocytosis was stopped by three washes in ice-cold PBS and fixation with paraformaldehyde. α_2-Macroglobulin was detected by using a sheep polyclonal antiserum (Biotrend, Cologne, Germany) and Cy2-coupled goat anti-sheep IgG (Jackson ImmunoResearch).

RESULTS

Characterization of Isoform-Specific Antibodies. We raised, in rabbits, polyclonal antibodies against seven different ClC-5 peptides. Affinity-purified sera directed against either an amino-terminal peptide (PEP5A) or a carboxyl-terminal peptide (PEP5E) recognized ClC-5 with high affinity in Western blots. ClC-5 is roughly 80% identical to the related ClC-3 and ClC-4 channels, and the peptides used to raise antibodies differ from their closest homologs by only a few amino acids. We tested the specificity of our antibodies in Western blots of *Xenopus* oocytes expressing ClC-3, ClC-4, or ClC-5. Although some sera had some cross-reactivity to ClC-4, this could be removed by affinity chromatography with the corresponding ClC-4 peptide, yielding highly isoform-specific antibodies (shown in Fig. 1*A* for PEP5A2 antibody). In Western blots of rat crude membrane preparations, both antibodies recognized a band of the correct size (about 80 kDa) in kidney (shown in Fig. 1*B* for PEP5E2). Both PEP5A2 and PEP5E2 antisera, which are directed against two nonoverlapping epitopes, were used in the present study. All structures described here were recognized by both antibodies.

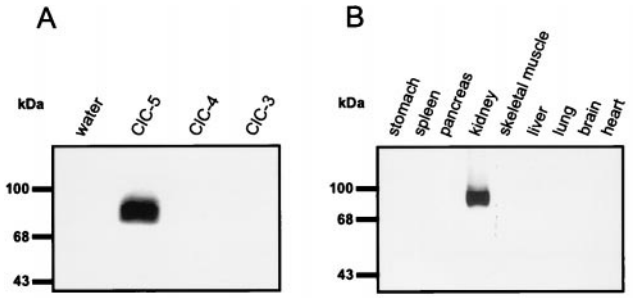

FIG. 1. Western blots of membranes from *Xenopus* oocytes expressing ClC-3, ClC-4, or ClC-5 (probed with PEP5A2) (*A*), and of crude membrane preparations from several rat organs (probed with PEP5E2) (*B*), demonstrating the specificity of the antibodies used in this work. Both sera specifically recognize a band of approximately 80 kDa in the kidney and in ClC-5-injected oocytes. This band corresponds to the predicted molecular mass of the ClC-5 chloride channel. The PEP5E2 antibody also recognized ClC-5 expressed in oocytes, and PEP5A2 recognizes the same band in kidney as the PEP5A2 antibody (not shown). On overexposure of additional blots (not shown), both antibodies also recognized a band in testis and faint bands in brain and liver. These tissues also express ClC-5 mRNA, albeit at a much lower level (4). All structures described in this study were observed with both antibodies, which were directed against two nonoverlapping epitopes, virtually excluding spurious results due to cross-reactivity.

ClC-5 in the Proximal Tubule: Colocalization with the Proton Pump and with Endocytosed Proteins. ClC-5 is found mainly in proximal tubules (Fig. 2), where expression starts in the S1 segment immediately at its exit from the glomerulus (Fig. 2*G*) and continues through the S2 and S3 segments with decreasing expression levels. ClC-5 is concentrated in a cytoplasmic "rim" apical to the nuclei (Fig. 2 *A* and *D*). Its expression is highest beneath the brush border, which can be specifically stained for villin, a cytoskeletal protein (Fig. 2*F*). Weak staining is seen throughout proximal tubular cells, including the brush border. The expression of ClC-5 largely overlaps with the vacuolar H^+-ATPase, which is overexpressed in proximal tubules (Fig. 2 *B* and *C*). Transmission electron microscopy shows the presence of immunoreactive material in vesicles that are concentrated below the microvilli of the brush border (Fig. 2 *J* and *K*). This specialized region contains an extensive endocytotic apparatus (9–11) necessary for the pronounced endocytotic activity of proximal tubule cells.

In Dent's disease, the excretion of β_2-microglobulin, which passes the glomerular filter and is normally reabsorbed in the proximal tubule (24), exceeds normal values 100- to 400-fold (8). We injected rats intravenously with fluorescently labeled β_2-microglobulin and fixed the kidneys by perfusion at various time points. Two minutes after injection, the reabsorbed protein largely overlaps with the sites of ClC-5 expression (Fig. 2 *D* and *E*). After 13 min the protein resides mainly in larger vesicles below the rim of maximal ClC-5 expression (Fig. 2 *G–I*).

ClC-5 in Intercalated Cells (ICs) of the Collecting Duct. ClC-5 is also expressed in cortical and medullary collecting ducts (Fig. 3). In contrast to proximal tubules, collecting ducts are composed of different cell types (for review, see ref. 25). Principal cells reabsorb sodium and secrete potassium, whereas ICs are involved in acid–base transport. The water channel aquaporin 2 is specifically expressed in principal cells and can be used to identify these cells (26). Double labeling with antibodies against aquaporin 2 and ClC-5 (Fig. 3*D*) reveals that ClC-5 (shown in red) is expressed mainly in ICs, which are interspersed between the principal cells, which specifically stain for aquaporin 2 (green). Acid–base transport

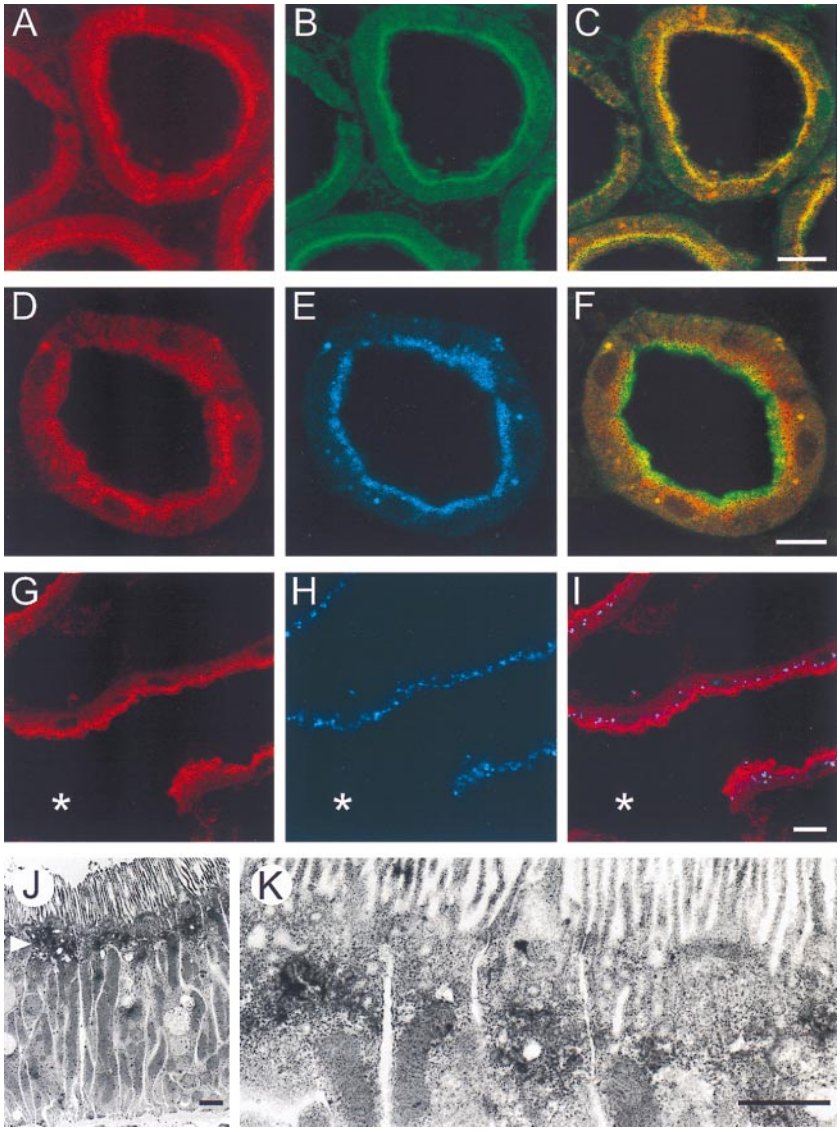

FIG. 2. Localization of the ClC-5 Cl^- channel in the proximal tubule of rat kidney by immunocytochemistry and laser scanning microscopy (*A–I*) or electron microscopy (*J* and *K*). (*A–C*) Cross section of several proximal tubules stained with the PEP5E2 antibody against ClC-5 (*A*) and with an antibody against the 70-kDa subunit of the H^+-ATPase (*B*). Both proteins are concentrated in a "rim" beneath the apical surface. *A* and *B* are merged in *C*. (*D–F*) Proximal tubule from a rat injected with Cy5-labeled β_2-microglobulin 2 min before fixation. The rim of ClC-5 expression (detected by PEP5E2 and shown in red in *D* and *F*) is located beneath the microvilli stained green with the anti-villin antibody in *F*. Low level expression of ClC-5 in other parts of the cell, including the brush border, cannot be excluded. The endocytosed protein shown in blue (*E*) largely overlaps with ClC-5 (*D*). (*G–I*) S1 segment of a proximal tubule immediately after its exit from the glomerular capsule (*), from a rat injected with Cy5-labeled β_2-microglobulin 13 min prior to fixation. As evident from the superimposed images (*I*), the reabsorbed protein (*H*) is generally deeper within the cells than the rim of maximal ClC-5 expression (detected with PEP5A2) (*G*). (*J* and *K*) Transmission electron micrographs showing the presence of ClC-5 (detected by PEP5E2 and peroxidase/diaminobenzidine) in a region rich in vesicles (indicated by the arrowhead) below the apical invaginations of the brush-border membrane. Two different proximal tubules are shown at different magnifications. (White bars indicate 10 μm; black bars, 1 μm.)

by ICs involves active proton pumping by a V-type H^+-ATPase. In acid-secreting α-ICs the H^+-ATPase is located apically. Transport of acid equivalents across the basolateral membrane occurs via band 3 (AE1), a chloride–bicarbonate exchanger (27, 28). β-ICs have a basolateral proton pump and consequently reabsorb acid. They lack the AE1 protein (the identity of the apical anion exchanger is unknown) (25). This classification is a simplification, in that a large proportion of the proton pump [and AE1 (29)] resides in vesicles and is inserted into the plasma membrane upon changes in the acid–base status (17, 30, 31).

In medullary collecting ducts, all ICs are of the α type. In these cells, ClC-5 is located apically and colocalizes with the apical H^+-ATPase. Cortical collecting ducts express both α- and β-ICs. ClC-5 is present in both cell types (Fig. 3 *A*, *C*, *E*, and *F*). ClC-5 expression overlaps with the apically located H^+-ATPase in the AE1-expressing α-ICs (indicated by arrows). Cells showing a diffuse apical cytoplasmic staining for the proton pump have a similar distribution of ClC-5 (arrowhead). Also in β-ICs (>), ClC-5 antibodies preferentially label the apical cell pole rather than completely overlapping with the mainly basolateral proton pump. Intracellular staining for ClC-5 is granular, particularly in β-ICs. In electron microscopy, ClC-5 antibodies intensely stain vesicles in the apical pole of ICs (Fig. 3 *G* and *H*), whereas the neighboring principal cells are unlabeled.

ClC-5 Is Present at the Plasma Membrane and in the Endocytotic Pathway of Transfected Cells. In transfected cells, ClC-5 resides in intracellular vesicles throughout the cytoplasm (Fig. 4 *A* and *B*). The plasma membrane is also labeled, often in dots. This may explain the plasma membrane chloride currents observed with *Xenopus* oocytes expressing ClC-5 (2, 4, 6, 7). When transfected COS-7 cells are allowed to take up α_2-macroglobulin by endocytosis, ClC-5 colocalizes with the protein in a large proportion of vesicles (Fig. 4 *B* and *C*). Transfection with the GTPase-deficient rab5 mutant Q79L leads to large vesicles that stain for rab5 (Fig. 4 *D–F*). These represent enlarged early endosomes (23). These structures stain intensely for ClC-5, which was cotransfected into COS-7 cells (Fig. 4*G*) or MDCK cells, a well differentiated epithelial cell line (Fig. 4*I*). Hence ClC-5 is targeted to early endosomes in both fibroblasts and epithelial cells. This targeting is incomplete, and some ClC-5 stayed at the plasma membrane (Fig. 4*G*). The homologous plasma membrane channel ClC-0 (22) is not directed to endosomes by coexpressing the rab5 mutant (Fig. 4 *E* and *H*), showing that this localization is specific for ClC-5.

DISCUSSION

Cellular and Subcellular Localization of the ClC-5 Cl^- channel. Every mammalian cell expresses a V-type H^+-

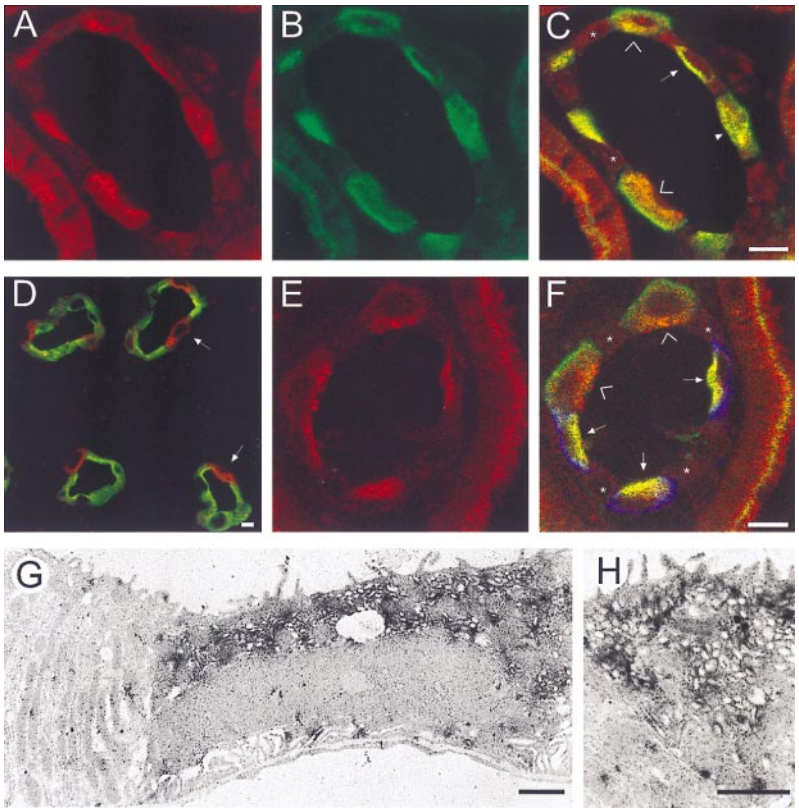

FIG. 3. ClC-5 in the collecting duct. (*A–C*) Cross section through a cortical collecting duct and part of a proximal tubule (left). (*A*) Staining for ClC-5 by the PEP5A2 antibody. (*B*) Staining for the H^+-ATPase by the E11 monoclonal antibody against the 31-kDa subunit. The two images are merged in C. The arrow indicates an α-IC (both proton pump and ClC-5 are apical), >s indicate β-ICs (pronounced basolateral H^+-ATPase and diffuse to apical ClC-5), and the arrowhead indicates a cell with diffuse cytoplasmic staining for both ClC-5 and the proton pump. (*D*) Cross section through the medulla; staining for aquaporin 2 (green) identifies principal cells of the collecting duct; between these are ICs (arrows), which stain red with PEP5A2 for ClC-5. (*E* and *F*) Cross section through a cortical collecting duct and longitudinal section through a proximal tubule (right). (*E*) Detection of ClC-5 (by PEP5E2). (*F*) Costaining for ClC-5 (red), the H^+-ATPase (green, by using the E11 monoclonal antibody), and the anion exchanger AE1 (blue). Costaining for ClC-5 and the H^+-ATPase appears yellow. Arrows indicate α-ICs (basolateral AE1, proton pump and ClC-5 both apical); >s indicate β-ICs, which lack AE1, have predominantly basolateral H^+-ATPase, and punctate apical staining for ClC-5. Asterisks (*) indicate principal cells. (*G* and *H*) Transmission electron micrographs stained for ClC-5 (by PEPE2). In *G*, an IC with stained apical cytoplasmic vesicles is shown with an adjacent unstained principal cell (left). (*H*) Higher magnification of the apical region of a different IC. (White bars, 10 μm; black bars, 1 μm.)

ATPase, which is necessary for the acidification of several intracellular organelles. In the kidney, two cell types, proximal tubule cells and ICs of the collecting duct, grossly overexpress the proton pump (17). It is exactly these cells that also overexpress the ClC-5 Cl^- channel. In the proximal tubules and in α-ICs, ClC-5 and the H^+-ATPase colocalize in the same subcellular regions. Expression of both proteins overlaps also in β-ICs, but the proton pump localizes preferentially to the basolateral region, whereas ClC-5 diffusely localizes to the apical cytoplasm.

Both proximal tubular cells and ICs are involved in acid–base transport and in endocytosis. Proximal tubule and α-ICs secrete acid equivalents into the tubular lumen, whereas β-ICs reabsorb acid. While acid secretion by proximal tubule cells is only partially due to the H^+-ATPase (it occurs mainly by means of an apical Na^+/H^+-exchanger), it occurs primarily by means of the H^+-ATPase in ICs. In those cells, acid secretion and reabsorption are regulated by the insertion and retrieval of proton pumps into apical and basolateral membranes, respectively (17, 30, 31). These processes occur by endo- and exocytosis. Most of the proton pump resides normally in intracellular vesicles. The diffuse intracellular staining of ICs with the ClC-5 antibody, the colocalization with the proton pump at the light microscopical level, and our immunoelectron microscopy strongly suggest that ClC-5 is present in proton-pump-containing vesicles. ICs also actively take up fluid-phase markers such as fluorescein-dextran (30, 32), but it is unknown whether this endocytotic activity is only a by-product of the insertional regulation of the proton pump.

In contrast, the pronounced endocytotic activity of proximal tubular cells serves a well defined role—i.e., the nearly quantitative reabsorption of proteins small enough to pass the glomerular filter (9–11). This high endocytotic activity correlates with a region beneath the brush border of proximal tubular cells, which is packed with endocytotic vesicles, endosomes, and recycling vesicles. The maximum of ClC-5 expression occurs exactly in this region. In the same region we also found endocytosed β_2-microglobulin, whose colocalization with ClC-5 was most significant at short times after uptake. Thus, if ClC-5 plays a role in the endocytotic pathway, it may be important for early rather than late steps. This conclusion is also supported by the colocalization with rab5, a marker of early endosomes, in transfected cells (Fig. 4).

ClC-5 was predominantly found in vesicular compartments within the cell, but it may also be expressed at the plasma membrane. This expression was most obvious in transfected cells. The immunocytochemistry of α-ICs also suggests a localization of ClC-5 at the apical membrane. However, the resolution of confocal laser microscopy is not sufficient to determine whether ClC-5 is located in the plasma membrane of renal tubular cells or whether it is exclusively present in vesicles just beneath the apical membrane. While it is clear that ClC-5 resides mainly in intracellular vesicles, cell surface expression seems necessary to explain the Cl^- currents observed in ClC-5-expressing oocytes (2, 4, 6, 7) and transfected cells (unpublished results).

Possible Roles of ClC-5 in Acid Transport and Endocytosis. The presence of ClC-5 in vesicles of the endocytotic pathway and, to a lesser extent, at the cell surface, suggests two hypotheses regarding ClC-5 function: First, ClC-5 may play a role at the cell surface, and its presence in endocytotic vesicles serves only to regulate its plasma membrane localization by endo- and exocytosis, analogous to proton pump regulation in ICs. Second, ClC-5 may function primarily in vesicles of the endocytotic pathway, and expression at the cell surface is just a by-product of vesicle recycling over the plasma membrane.

These hypotheses are not mutually exclusive. The colocalization with the proton pump suggests that ClC-5 serves as a conductive pathway for the electroneutral transport of acid. This may occur both within vesicles and at the plasma membrane. Indeed, Cl^- channels have been observed in ICs, although apical Cl^- channels were primarily found in β-ICs (25). The properties of these, however, seem to differ from those of ClC-5 expressed in *Xenopus* oocytes (4). Although intracellular Cl^- is normally well above the electrochemical equilibrium across the apical membrane, there has also be

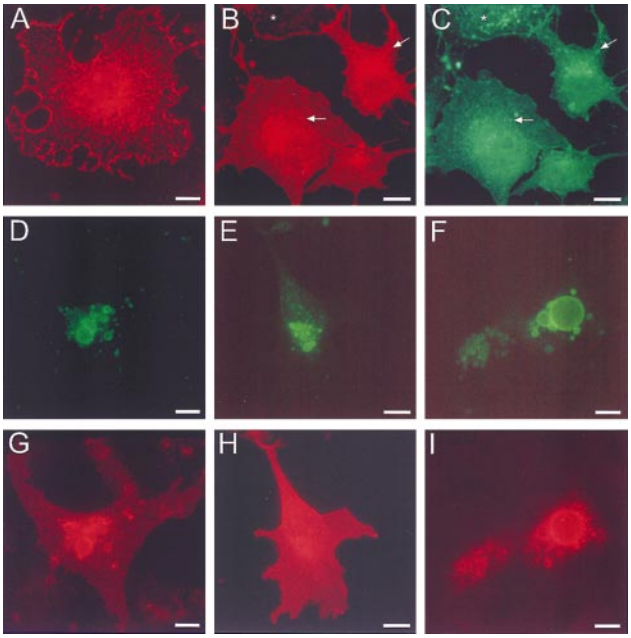

FIG. 4. ClC-5 in transfected cells. COS-7 (*A–E*, *G*, and *H*) or MDCK (*F* and *I*) cells were transfected with ClC-5 (*A–D*, *F*, *G*, and *I*), or, as a control, with ClC-0 (*E* and *H*). ClC-5 (detected by PEP5A2) is expressed in vesicles throughout the cytoplasm and in a punctate pattern at the plasma membrane (*A* and *B*). Cells in *B* and *C* were allowed to endocytose α_2-macroglobulin and examined in double-immunofluorescence for ClC-5 (red) (*B*) and α_2-macroglobulin (green) (*C*). There is a large degree of colocalization as indicated by arrows for some arbitrarily chosen vesicles. A cell not transfected with ClC-5 (*) has also internalized α_2-macroglobulin. Cells in *D–I* were cotransfected with the GTPase-deficient rab5 mutant Q79L tagged with a myc epitope. Staining for this epitope (green) (*D–F*) reveals large vesicles representing enlarged early endosomes. These costain for ClC-5 both in COS-7 cells (*G*) and in MDCK cells that have been grown to an epithelial layer (*I*). In contrast, when cotransfected with the homologous ClC-0 channel (*E* and *H*), ClC-0 is excluded from these vesicles (stained for rab5 in *E*) and stays in the plasma membrane (as detected with the T12 antibody and shown in red in H). (Bars = 10 μm.)

some speculation that Cl^- channels are inserted together with the H^+-ATPase into the apical membrane of proximal tubular cells (30, 33).

To explain the proteinuria in Dent's disease, a role of ClC-5 in the acidification of vesicles in the endocytotic pathway is much more attractive (3, 4, 34). Many intracellular organelles are acidified by H^+-ATPases (13, 17). Along the endocytotic pathway, intravesicular pH gets increasingly acidic on the way from endocytotic vesicles to early and late endosomes and finally to lysosomes, whose internal pH is roughly 5.0 to 5.5.

Acidification in the endocytotic pathway is required for receptor–ligand interactions and several sorting events (35–37). Inhibition of endosome acidification, either by inhibiting the H^+-ATPase or by dissipating the pH gradient, severely interferes with the function of the endocytotic pathway. It leads, e.g., to a slowed endocytotic recycling and intracellular retention of recycling receptors (36, 38), to an impaired retrieval of trans-Golgi network proteins from the cell surface (39), and to a defective intracellular transport of endocytosed markers (14, 15). This interference may occur at different steps in the endocytotic pathway, possibly depending on the cell type (14, 15, 40, 41). Endosomal alkalinization reduces endocytosis of albumin in OK cells, a renal proximal tubular cell line (16), and CHO cell mutants impaired in endocytosis have defects in endosomal acidification (42, 43). Thus, there is compelling evidence that endosomal acidification is required for the overall process of endocytosis.

The V-type H^+-ATPase is electrogenic: by pumping H^+, it transports both acid equivalents and electric charge (17). Acid equivalents are buffered more efficiently than the electric charge, which is "buffered" by the membrane capacitance of the vesicle. As a consequence, the inside-positive voltage across the vesicle membranes will energetically limit the pH gradient achievable by ATP hydrolysis. Efficient pumping requires a parallel conductance, leading to an overall electroneutral transport. In several vesicle preparations, acidification depends on the presence of cytoplasmic anions, suggesting the presence of a Cl^- conductance (18–20). Acidification of endosomes from renal proximal tubules is stimulated by anions, with chloride being more efficient than iodide (18). This observation agrees well with the $Cl^- > I^-$ selectivity of the ClC-5 Cl^- channel (4).

The molecular identity of the Cl^- channel(s) involved in endosomal acidification has remained elusive. Our work suggests that the ClC-5 Cl^- channel could be such a rate-limiting Cl^- channel in renal proximal tubule endosomes. This suggestion is based on the presence of ClC-5 in endosomes, its colocalization with endocytosed protein and the H^+-ATPase in the proximal tubule, the known requirement of endosomal acidification for endocytosis, and, finally, the proteinuria observed in Dent's disease. The selective urinary increase in low molecular weight proteins points to a specific defect in protein reabsorption by the proximal renal tubule, the predominant site of ClC-5 expression. Patients with Dent's disease provide a "knock-out" model for the ClC-5 Cl^- channel. Indeed, all Dent's disease mutations analyzed in the *Xenopus* oocyte expression system either abolished or largely reduced Cl^- currents (2, 6, 7).

While this observation suggests that ClC-5 may be rate limiting for endocytosis in the proximal tubule, it cannot play a universal role in endocytosis. If it did, mutations in ClC-5 would be lethal. Because ClC-5 is expressed in a highly specific manner, different Cl^- channels may play similar roles in other cells and organelles. Other Cl^- channels such as CFTR were also proposed to be important for membrane trafficking (44), but this is controversial (45). We suggest that other CLC Cl^- channels will turn out to play similar roles.

Indirect support for a role of CLC channels in acidifying intracellular compartments comes also from yeast: disruption of either the yeast CLC (*GEF1*) (46), which resides in intracellular vesicles (47) recently shown to be a Golgi compartment (48, 49), or of *GEF2* (*VMA3*), a subunit of the vacuolar H^+-ATPase, causes identical phenotypes (46). This includes a sensitivity to more alkaline pH (48, 49), consistent with a role of yeast CLC in acidification. In mammals, ClC-3 and ClC-4 may have functions similar to ClC-5, although ClC-3 was proposed to be a swelling-activated channel (50). These proteins are about 80% identical to ClC-5 and more broadly expressed (5). Partially overlapping expression patterns may explain why there is no urinary acidification defect in Dent's disease despite the prominent ClC-5 expression in ICs. *In situ* hybridization revealed that ClC-3 is also expressed in β-ICs (51). Surprisingly, that study detected ClC-5 mRNA only in α-, not in β-, ICs, and it failed to detect ClC-5 message in the proximal tubule.

The mechanism by which ClC-5 disruption leads to kidney stones is unknown and may be complex. For instance, hypercalciuria may be secondary to a loss of regulatory proteins normally reabsorbed in the kidney, or a trafficking defect may change the localization of other channels or transporters.

In summary, ClC-5 is expressed mainly in intracellular vesicles both in endocytotically active kidney cells and in transfected cells. Our data suggest that ClC-5 may be rate limiting for the acidification of endocytotic compartments in the proximal tubule, leading to the proteinuria observed in Dent's disease. We propose that the diversity of endocytotic processes, or more generally of intracellular vesicle trafficking,

may be reflected in a molecular diversity not only of H^+-ATPase subunits (17) but also of intracellular Cl^- channels.

We thank D. Drenckhahn for the anti-band 3 antibody, S. Gluck for the E11 mouse monoclonal anti-31-kDa subunit and the rabbit anti-56-kDa subunit H^+-ATPase antibodies, M. Knepper for the anti-aquaporin 2 antibody, S. Robine and D. Louvard for the anti-villin antibody, K. Steinmeyer for the ClC-0 antibody, and D. Stone for the anti-70-kDa subunit H^+-ATPase antibody. We also thank M. Schweizer for advice on immunocytochemistry, R. Witzgall for help with kidney fixation, and B. Merz, C. Büttgen, and C. Neff for excellent technical assistance. This work was supported by grants from the Deutsche Forschungsgemeinschaft and the Fonds der Chemischen Industrie to T.J.J.

1. Wrong, O. M., Norden, A. G. W. & Fest, T. G. (1994) *Q. J. Med.* **87,** 473–493.
2. Lloyd, S. E., Pearce, S. H., Fisher, S. E., Steinmeyer, K., Schwappach, B., Scheinman, S. J., Harding, B., Bolino, A., Devoto, M., Goodyer, P., *et al.* (1996) *Nature (London)* **379,** 445–449.
3. Fisher, S. E., Black, G. C., Lloyd, S. E., Hatchwell, E., Wrong, O., Thakker, R. V. & Craig, I. W. (1994) *Hum. Mol. Genet.* **3,** 2053–2059.
4. Steinmeyer, K., Schwappach, B., Bens, M., Vandewalle, A. & Jentsch, T. J. (1995) *J. Biol. Chem.* **270,** 31172–31177.
5. Jentsch, T. J., Günther, W., Pusch, M. & Schwappach, B. (1995) *J. Physiol. (London)* **482,** 19S–25S.
6. Lloyd, S. E., Pearce, S. H., Günther, W., Kawaguchi, H., Igarashi, T., Jentsch, T. J. & Thakker, R. V. (1997) *J. Clin. Invest.* **99,** 967–974.
7. Lloyd, S. E., Günther, W., Pearce, S. H., Thomson, A., Bianchi, M. L., Bosio, M., Craig, I. W., Fisher, S. E., Scheinman, S. J., Wrong, O., *et al.* (1997) *Hum. Mol. Genet.* **6,** 1233–1239.
8. Reinhart, S. C., Norden, A. G., Lapsley, M., Thakker, R. V., Pang, J., Moses, A. M., Frymoyer, P. A., Favus, M. J., Hoepner, J. A. & Scheinman, S. J. (1995) *J. Am. Soc. Nephrol.* **5,** 1451–1461.
9. Maack, T., Johnson, V., Kau, S. T., Figueiredo, J. & Sigulem, D. (1979) *Kidney Int.* **16,** 251–270.
10. Christensen, E. I. & Nielsen, S. (1991) *Semin. Nephrol.* **11,** 414–439.
11. Christensen, E. I., Nielsen, S., Moestrup, S. K., Borre, C., Maunsbach, A. B., de Heer, E., Ronco, P., Hammond, T. G. & Verroust, P. (1995) *Eur. J. Cell Biol.* **66,** 349–364.
12. Mellman, I. (1996) *Annu. Rev. Cell Dev. Biol.* **12,** 575–625.
13. Mellman, I., Fuchs, R. & Helenius, A. (1986) *Annu. Rev. Biochem.* **55,** 663–700.
14. Clague, M. J., Urbé, S., Aniento, F. & Gruenberg, J. (1994) *J. Biol. Chem.* **269,** 21–24.
15. van Weert, A. W. M., Dunn, K. W., Geuze, H. J., Maxfield, F. R. & Stoorvogel, W. (1995) *J. Cell Biol.* **130,** 821–834.
16. Gekle, M., Mildenberger, S., Freudinger, R. & Silbernagl, S. (1995) *Am. J. Physiol.* **268,** F899–F906.
17. Gluck, S. L., Underhill, D. M., Iyori, M., Holliday, L. S., Kostrominova, T. Y. & Lee, B. S. (1996) *Annu. Rev. Physiol.* **58,** 427–445.
18. Sabolic, I. & Burckhardt, G. (1986) *Am. J. Physiol.* **250,** F817–F826.
19. Fuchs, R., Male, P. & Mellman, I. (1989) *J. Biol. Chem.* **264,** 2212–2220.
20. van Dyke, R. W. (1988) *J. Biol. Chem.* **263,** 2603–2611.
21. Jordt, S.-E. & Jentsch, T. J. (1997) *EMBO J.* **16,** 1582–1592.
22. Jentsch, T. J., Steinmeyer, K. & Schwarz, G. (1990) *Nature (London)* **348,** 510–514.
23. Stenmark, H., Parton, R. G., Steele-Mortimer, O., Lütcke, A., Gruenberg, J. & Zerial, M. (1994) *EMBO J.* **13,** 1287–1296.
24. Sundin, D. P., Cohen, M., Dahl, R., Falk, S. & Molitoris, B. A. (1994) *Am. J. Physiol.* **267,** F380–F389.
25. Schuster, V. L. (1993) *Annu. Rev. Physiol.* **55,** 267–288.
26. Nielsen, S., DiGiovanni, S. R., Christensen, E. I., Knepper, M. A. & Harris, H. W. (1993) *Proc. Natl. Acad. Sci USA* **90,** 11663–11667.
27. Drenckhahn, D., Schluter, K., Allen, D. P. & Bennett, V. (1985) *Science* **230,** 1287–1289.
28. Alper, S. L., Natale, J., Gluck, S., Lodish, H. F. & Brown, D. (1989) *Proc. Natl. Acad. Sci. USA* **86,** 5429–5433.
29. Madsen, K. M., Kim, J. & Tisher, C. C. (1992) *Am. J. Physiol.* **262,** F1015–F1022.
30. Schwartz, G. J. & Al-Awqati, Q. (1985) *J. Clin. Invest.* **75,** 1638–1644.
31. Bastani, B., Purcell, H., Hemken, P., Trigg, D. & Gluck, S. (1991) *J. Clin. Invest.* **88,** 126–136.
32. Lencer, W. I., Weyer, P., Verkman, A. S., Ausiello, D. A. & Brown, D. (1990) *Am. J. Physiol.* **258,** C309–C317.
33. Aronson, P. S. & Giebisch, G. (1997) *Am. J. Physiol.* **273,** F179–F192.
34. Hebert, S. C. (1996) *Nature (London)* **379,** 398–399.
35. Dautry-Varsat, A., Ciechanover, A. & Lodish, H. F. (1983) *Proc. Natl. Acad. Sci. USA* **80,** 2258–2262.
36. Presley, J. F., Mayor, S., McGraw, T. E., Dunn, K. W. & Maxfield, F. R. (1997) *J. Biol. Chem.* **272,** 13929–13936.
37. Tycko, B. & Maxfield, F. R. (1982) *Cell* **28,** 643–651.
38. Johnson, L. S., Dunn, K. W., Pytowski, B. & McGraw, T. E. (1993) *Mol. Biol. Cell* **4,** 1251–1266.
39. Chapman, R. E. & Munro, S. (1994) *EMBO J.* **13,** 2305–2312.
40. D'Arrigo, A., Bucci, C., Toh, B. H. & Stenmark, H. (1997) *Eur. J. Cell Biol.* **72,** 95–103.
41. van Deurs, B., Holm, P. K. & Sandvig, K. (1996) *Eur. J. Cell Biol.* **69,** 343–350.
42. Roff, C. F., Fuchs, R., Mellman, I. & Robbins, A. R. (1986) *J. Cell Biol.* **103,** 2283–2297.
43. Yamashiro, D. J. & Maxfield, F. R. (1987) *J. Cell Biol.* **105,** 2723–2733.
44. Bradbury, N. A., Jilling, T., Berta, G., Sorscher, E. J., Bridges, R. J. & Kirk, K. L. (1992) *Science* **256**, 530–532.
45. Dunn, K. W., Park, J., Semrad, C. E., Gelman, D. L., Shevell, T. & McGraw, T. E. (1994) *J. Biol. Chem.* **269,** 5336–5345.
46. Greene, J. R., Brown, N. H., DiDomenico, B. J., Kaplan, J. & Eide, D. J. (1993) *Mol. Gen. Genet.* **241,** 542–553.
47. Hechenberger, M., Schwappach, B., Fischer, W. N., Frommer, W. B., Jentsch, T. J. & Steinmeyer, K. (1996) *J. Biol. Chem.* **271,** 33632–33638.
48. Gaxiola, R. A., Yuan, D. S., Klausner, R. D. & Fink, G. R. (1998) *Proc. Natl. Acad. Sci. USA* **95,** 4046–4050.
49. Schwappach, B., Stobrawa, S., Hechenberger, M., Steinmeyer, K. & Jentsch, T. J. (1998) *J. Biol. Chem.* **273,** 15110–15118.
50. Duan, D., Winter, C., Cowley, S., Hume, J. R. & Horowitz, B. (1997) *Nature (London)* **390,** 417–421.
51. Obermüller, N., Gretz, N., Kriz, W., Reilly, R. F. & Witzgall, R. (1998) *J. Clin. Invest.* **101,** 635–642.